The possibility of determining the spin-orbit interaction constants using scanning tunneling microscopy

N. V. KhotkevychN. R. VovkYu. A. Kolesnichenko

Citation: Low Temp. Phys. **42**, (2016); doi: 10.1063/1.4948444
View online: http://dx.doi.org/10.1063/1.4948444
View Table of Contents: http://aip.scitation.org/toc/ltp/42/4
Published by the American Institute of Physics

The possibility of determining the spin-orbit interaction constants using scanning tunneling microscopy

N. V. Khotkevych

B. Verkin Physics and Technology Institute for Low Temperatures, NAS Ukraine, 47 Nauka Ave., Kharkov 61103, Ukraine

N. R. Vovk

V. N. Karazin Kharkov National University, 4 Svoboda Sq., Kharkov 61022, Ukraine and B. Verkin Physics and Technology Institute for Low Temperatures, NAS Ukraine, 47 Nauka Ave., Kharkov 61103, Ukraine

Yu. A. Kolesnichenko[a)]

B. Verkin Physics and Technology Institute for Low Temperatures, NAS Ukraine, 47 Nauka Ave., Kharkov 61103, Ukraine

(Submitted January 14, 2016)
Fiz. Nizk. Temp. **42**, 387–397 (April 2016)

A study of electron tunneling from quasi-two-dimensional (surface) states with spin-orbit interaction into bulk-mode states, within the framework of a model of an infinitely thin inhomogeneous tunnel magnetic barrier between two conductors. We analyze how the scattering of quasi-two-dimensional electrons on a single magnetic defect affects the tunneling current in this system. We also obtain an analytical expression for the conductance of the tunnel point-contact, as a function of its distance from the defect. It is shown that analyzing local magnetization oscillations around the defect using spin-polarized scanning tunneling microscopy allows us to determine the spin-orbit interaction constant. *Published by AIP Publishing.* [http://dx.doi.org/10.1063/1.4948444]

Introduction

Interest in the study of spin-orbit interaction (SOI) in a two-dimensional electron gas (2DEG) is fueled by the fact that SOI manifests itself as a diverse range of physical phenomena,[1,2] and that it has many promising practical applications in an emerging field of quantum electronics—spintronics.[3] Two-dimensional (2D) electron (and hole) systems can be created artificially (semiconducting heterostructures with quantum wells, delta-doped semiconductors, electrons on the surface of liquid helium), or they are the properties of certain physical systems (graphene, thin films).

One example of 2DEG with SOI is surface electron states in metals.[4] In contrast to isolated two-dimensional conducting systems in heterostructures, surface states cannot be studied using galvanomagnetic measurements due to their high bulk conductivity. However they can be detected and studied using methods that are sensitive to the electron structure of the surface layer of a conductor. Therefore, in Refs. 5–7, spin-orbit splitting of the spectrum of surface states near the surface (111) of precious metals was detected using angle-resolved photoemission spectroscopy.

Scanning tunneling microscopy (STM)[8] is an effective method of studying conductor surfaces. In a study authored by Tersoff and Hamann,[9] it was shown that the STM-measured conductance between the atomically sharp contact and the test sample is proportional to the local density of states (LDS) at the point located directly beneath the contact. This result determined how one branch of STM development is applied.[10] Spin-polarized scanning tunneling microscopy (SP-STM) allows us to study the surface magnetic structures with an atomic resolution.[11,12] In Ref. 13 it was shown that the SP-STM current contains an additional term that is proportional to the scalar product of the magnetization vector of the STM contact and the vector of the local magnetization density (LMD) of the sample. Therefore, the spin-polarized scanning tunneling microscopy is a method for determining local magnetic characteristics of the surface.

Additional possibilities for obtaining information about the electron energy spectrum come to us from studying the oscillations of the density of states (Friedel oscillations[14]) in the vicinity of the point defects on the surface.[15] In particular, the STM analysis of the image around the defect allows us to recreate the Fermi-contour of two-dimensional surface states.[16–18] If the defect has a magnetic moment, in addition to Friedel oscillations, magnetization oscillations are generated by the electron spin polarization (RKKY spin polarization)[19] around the defect. In Ref. 20, SP-STM was used to reveal how the magnetic state of nano Co islands on the surface of Cu (111), affects the oscillations observed in the STM conductance, which were occurring on the islands themselves and around them.

A significant number of experimental and theoretic studies (see Refs. 21–30 and references therein) are dedicated to studying quantum interference effects in 2D electron scattering by a point defect with SOI. However, there is still undoubted interest in obtaining analytical formulas for SP-STM conductance, which would allow us to analyze its dependence on STM distance between the contact and the defect, the magnitude and direction of the magnetic moment of the defect, the SOI constants and the energy spectrum parameters of the charge carriers, in explicit form. Although similar results can be obtained only within the framework of

considerably simplified models, they often turn out to be crucial in the physical interpretation of the data obtained in the experiment.

In this study we examined the problem of conductance G of the tunnel point-contact in the case of electron tunneling between the bulk states and those states localized around the interface (surface) with Rashba SOI.[31] The manifestation of quantum interference effects in the contact conductance, caused by the scattering of electrons by the magnetic point defect, is examined.

The model of an inhomogeneous δ-barrier[32] is generalized by us for a case of a magnetic dielectric layer between conductors. An analytical expression for the contact conductance is obtained in an approximation with low tunneling barrier transparency and in the Born approximation for electron scattering by a defect. The connection between the conductance and the local density of states and local magnetization around the defect, is established. The value of G is analyzed as a function of the parameters that characterize 2DEG and the defect. The possibilities of obtaining information about SOI in 2DEG in experiments using SP-STM, is discussed.

1. Model of an inhomogeneous magnetic tunneling junction

One of the models used to describe STM experiments is the model of an inhomogeneous δ-barrier that describes the tunneling current through a small area of the interface that divides two conductors. This model was first considered in Ref. 32, in which it was shown that in the limit approaching infinity of the amplitude $U_0 \to \infty$ of the barrier with an arbitrary shape between two conducting half-spaces, the tunneling resistance can be found as asymptotically exact.

In a number of studies (see overview in Ref. 33) the model of the δ-barrier is used to describe the influence of single point defects under the conductor surface, on the conductance of the tunnel point-contact, measured using STM. In particular, the problem of tunneling between ferromagnetic and nonmagnetic metals in the presence of a magnetic cluster close to the contact, was considered.[34] As a result, the applicability of this model to the description of electron tunneling from (three-dimensional) bulk states to quasi-two-dimensional surface states, for sufficiently small areas of a transparent barrier, has been proved.[35,36]

The model used when solving this problem is shown in Fig. 1. Two conductive half-spaces are divided by a magnetic dielectric barrier that is impenetrable to electrons. The barrier has a small area (with a typical radius a) with ultimate transparency (contact). In the half-space $z < 0$ there exist electron states with spin-orbit interaction, which are localized close to the boundary. At a distance of $\mathbf{r}_0$ from the center of the tunneling region $\mathbf{r} = 0$, which is z_0 from the interface, there is a short-range magnetic defect that has a spin of $S \geq 1$, and is less than the attenuation depth of the "surface" states $l_{\text{surf}} \gg a$. The former condition ensures the absence of a full screening of the magnetic moment of the defect by electrons (Kondo effect), even at $T = 0$.[37] We think that the only reason the electron scatter occurs is due to their elastic interaction with the defect. We assume the temperature is about equal to zero. A sufficiently small voltage V is applied to the system. We will calculate the current using an approximation that is linear with respect to V, to be

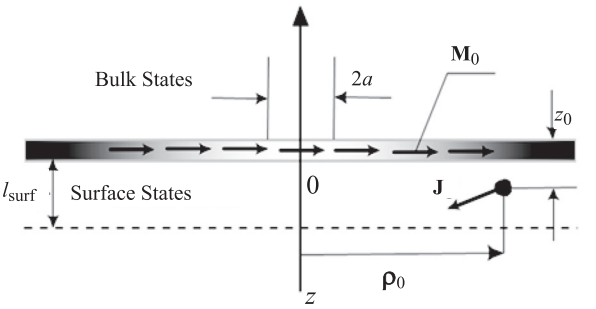

FIG. 1. A model depicting an inhomogeneous magnetic tunneling barrier. The arrows represent the direction of the barrier magnetization vector $\mathbf{M}_0$, and the magnetic moment of the defect, $\mathbf{J}$.

specific when the tunneling occurs from the "surface" states to the bulk states.

The magnetic δ-barrier between metals will be described using the potential

$$\hat{U}(\mathbf{r}) = (\hat{\sigma}_0 - \mathbf{M}_0\hat{\boldsymbol{\sigma}})U_0 f(\boldsymbol{\rho})\delta(z), \tag{1}$$

wherein $\mathbf{M}_0$ is the dimensionless (normalized to the amplitude of the barrier U_0) vector of tunnel barrier magnetization, $M_0 \ll 1$, $\hat{\boldsymbol{\sigma}} = (\hat{\sigma}_x, \hat{\sigma}_y, \hat{\sigma}_z)$ is the Pauli vector, $\hat{\sigma}_0$ is the unit 2×2 matrix. The function $f(\boldsymbol{\rho})$ of the two-dimensional vector $\boldsymbol{\rho} = (x,y)$ in the plane of the barrier boundary $z = 0$ fulfills the condition

$$f(\boldsymbol{\rho}) = \begin{cases} \sim 1, & \rho \lesssim a, \\ \to \infty, & \rho \gg a, \end{cases} \tag{2}$$

in which a is the typical size of the tunneling region (of the contact). Hereinafter we will assume that the radius a is sufficiently small, and that the following inequality is fulfilled[35]

$$\frac{\hbar^2 k_F a^2}{m^* U_0 l_{\text{surf}}^2} \ll 1, \tag{3}$$

wherein $k_F = \frac{1}{\hbar}\sqrt{2m^*\varepsilon_F}$ is the Fermi wave vector, ε_F is the Fermi energy, m^* is the effective electron mass. Inequality (3) ensures that the perturbation theory is applicable in solving this problem.

For $z \geq 0$ the wave functions $\hat{\Psi}^{(+)}(\rho, z)$ satisfy the Schrödinger equation for free electrons with an effective mass m^* and energy ε

$$\frac{\hat{\mathbf{p}}^2}{2m^*}\hat{\Psi}^{(+)}(\boldsymbol{\rho}, z) = \varepsilon\hat{\Psi}^{(+)}(\boldsymbol{\rho}, z), \tag{4}$$

wherein $\hat{\mathbf{p}} = i\hbar\nabla$ is the momentum operator.

In the half-space $z < 0$, the Schrödinger equation looks like

$$\left[\frac{\hat{\mathbf{p}}^2}{2m^*}\hat{\sigma}_0 + \hat{H}_{SO} + \hat{D}(\boldsymbol{\rho}, z) + \hat{\sigma}_0 V_{\text{surf}}(z)\right]\hat{\Psi}^{(-)}(\boldsymbol{\rho}, z) = \varepsilon\hat{\Psi}^{(-)}(\boldsymbol{\rho}, z). \tag{5}$$

In Equation (5), $\hat{H}_{SO}$ is the SOI Hamiltonian. The $\hat{D}(\boldsymbol{\rho}, z)$ term describes the interaction of the electrons with the magnetic defect, that is simulated by the point potential

$$\hat{D}(\boldsymbol{\rho}, z) = (g\hat{\sigma}_0 + \mathbf{J}\hat{\boldsymbol{\sigma}})\delta(\boldsymbol{\rho} - \boldsymbol{\rho}_0)\delta(z - z_0), \tag{6}$$

wherein g is the constant of the potential electron interaction with the defect, $\mathbf{J}$ is the effective magnetic moment of the alloy, with a spin $S \geq 1$, $\mathbf{J} = J_{ex}\langle \mathbf{S} \rangle$, wherein J_{ex} is the constant of exchange interaction of the electron and the defect, $\langle \mathbf{S} \rangle$ is the intrinsic magnetic moment of the defect, based on a partial screening of the conduction electrons. We assume that the direction of the $\mathbf{J}$ vector is fixed, and do not consider the processes of revolution and precession of the defect spin. The potential $V_{surf}(z)$ leads to the appearance of a related (surface) state in the $z<0$ region, near the interface. Hereinafter the specific form of the potential $V_{surf}(z)$ in Equation (5) is not significant.

The wave functions $\hat{\Psi}^{(\pm)}(\boldsymbol{\rho}, z)$ are related to the δ-barrier via the standard terms of continuity and discontinuity of the normal derivative

$$\hat{\Psi}^{(+)}(\boldsymbol{\rho}, +0) = \hat{\Psi}^{(-)}(\boldsymbol{\rho}, -0), \tag{7}$$

$$\frac{\partial}{\partial z}\hat{\Psi}^{(+)}(\boldsymbol{\rho}, z = +0) - \frac{\partial}{\partial z}\hat{\Psi}^{(-)}(\boldsymbol{\rho}, z = -0) = \frac{2m*}{\hbar^2}U_0(\hat{\sigma}_0 - \mathbf{M}_0\hat{\boldsymbol{\sigma}})f(\boldsymbol{\rho})\hat{\Psi}^{(\pm)}(\boldsymbol{\rho}, 0). \tag{8}$$

2. The calculation of tunneling current

Further analytical calculations demand additional assumptions. Following the procedure proposed in Ref. 32, the wave functions $\hat{\Psi}^{(\pm)}(\boldsymbol{\rho}, z)$ in the half spaces $z > 0$ and $z < 0$ will be sought in the form of an expansion in powers of $1/U_0$. Since it is enough to know the wave function of the electrons passing through the barrier $\hat{\Psi}^{(\pm)}_{tr}(\rho, z)$ to calculate the tunneling current, we will write the expansion of the function $\hat{\Psi}^{(\pm)}(\boldsymbol{\rho}, z)$ as follows:

$$\hat{\Psi}^{(\pm)}(\boldsymbol{\rho}, z) = \hat{\Psi}^{(\pm)}_1(\boldsymbol{\rho}, z) \equiv \hat{\Psi}^{(\pm)}_{tr}(\boldsymbol{\rho}, z), \tag{9}$$

$$\hat{\Psi}^{(-)}(\boldsymbol{\rho}, z) = \hat{\Psi}^{(-)}_0(\boldsymbol{\rho}, z) + \hat{\Psi}^{(-)}_1(\boldsymbol{\rho}, z), \tag{10}$$

wherein $\hat{\Psi}^{(\pm)}_1 \sim 1/U_0$. For $U \to \infty$ from the boundary condition of (7) we have

$$\hat{\Psi}^{(-)}_0(\boldsymbol{\rho}, 0) = 0, \quad \hat{\Psi}^{(+)}_0(\boldsymbol{\rho}, z) + \hat{\Psi}^{(-)}_1(\boldsymbol{\rho}, z). \tag{11}$$

In the zeroth-order approximation with respect to $1/U_0$ the boundary condition for $\hat{\Psi}^{(+)}_{tr}(\boldsymbol{\rho}, z)$ obtains the shape

$$-\frac{\partial}{\partial_z}\hat{\Psi}^{(-)}_0(\boldsymbol{\rho}, z = -0) = \frac{2m^*}{\hbar^2}U_0(\hat{\sigma}_0 - \mathbf{M}_0\hat{\boldsymbol{\sigma}})f(\boldsymbol{\rho})\hat{\Psi}^{(+)}_1(\boldsymbol{\rho}, 0), \quad s = 1, 2. \tag{12}$$

Therefore the problem of finding $\hat{\Psi}^{(+)}_{tr}(\boldsymbol{\rho}, z)$ reduces to solving two simpler equations: solving the Schrödinger equation (5) with a zero boundary condition $\hat{\Psi}^{(-)}_0(\boldsymbol{\rho}, 0) = 0$, and solving the Schrödinger equation for free electrons (4) for the function $\hat{\Psi}^{(+)}_1(\boldsymbol{\rho}, z)$ with the given condition (12) at the interface $\hat{\Psi}^{(+)}_1(\boldsymbol{\rho}, 0)$. As a result of calculations that are similar to those conducted in Refs. 35 and 38, and accounting for $M_0 \ll 1$, we get

$$\hat{\Psi}^{(+)}_{tr}(\boldsymbol{\rho}, z) = -\frac{\hbar^2(\sigma_0 + \mathbf{M}_0\hat{\boldsymbol{\sigma}})}{2(2\pi)^2 m * U_0} \times \int_{-\infty}^{\infty} d\boldsymbol{\kappa}' \int_{-\infty}^{\infty} \frac{d\boldsymbol{\rho}'}{f(\boldsymbol{\rho}')}\frac{\partial}{\partial z} \times \left[\Psi^{(-)}_0(\boldsymbol{\rho}', z)\right]_{z=-0} e^{i\boldsymbol{\kappa}'(\boldsymbol{\rho}-\boldsymbol{\rho}')+iz\sqrt{k^2-\kappa'^2}}. \tag{13}$$

Equation (5) with the boundary condition (11) is solved according to the scattering potential perturbation theory $\hat{D}(\boldsymbol{\rho}, z)$, which we believe to be sufficiently small, and will therefore limit ourselves to the linear (Born) approximation with respect to $\hat{D}(\boldsymbol{\rho}, z)$

$$\hat{\Psi}^{(-)}_0(\boldsymbol{\rho}, z) = \hat{\Psi}^{(-)}_{00}(\boldsymbol{\rho}, z) + \hat{\Psi}^{(-)}_{01}(\boldsymbol{\rho}, z). \tag{14}$$

For $\hat{D}(\boldsymbol{\rho}, z) = 0$, the variables in Equation (5) can be separated and its solution can be represented as a product

$$\hat{\Psi}^{(-)}_{00}(\boldsymbol{\rho}, z) = \hat{\psi}^{(00)}(\boldsymbol{\rho})\chi_0(z), \quad z \leq 0, \tag{15}$$

in which $\hat{\Psi}^{(00)}(\boldsymbol{\rho})$ is the wave function of the two-dimensional electron gas with SOI. The wave function that describes the motion of the electron along the normal to the interface $\chi(z, \varepsilon_\perp)$, is the solution to equation

$$\frac{\hbar^2}{2m^*}\frac{\partial^2\chi(z)}{\partial z^2} + (\varepsilon_\perp - V_{surf}(z))\chi(z) = 0, \quad z \leq 0, \tag{16}$$

normalized, and satisfies the boundary conditions

$$\chi(0) = 0, \quad \chi(z \to \infty) \to 0, \tag{17}$$

and the spectrum of eigenvalues of Equation (16) is discrete. We assume that in the energy region that is of interest to us, which is less than the Fermi energy ε_F, there is only one discrete level $\varepsilon_\perp = \varepsilon_0$. If $V_{surf}(z)$ is a monotonically increasing analytic function, then we can always select the solution $\chi_0(z) = \chi(z, \varepsilon_0)$ as being real.[39]

The eigenvalues of the energy $E_{1,2}$, that correspond to the wave functions (15) are equal to

$$E_{1,2}(\boldsymbol{\kappa}) = \varepsilon_{1,2}(\boldsymbol{\kappa}) + \varepsilon_0, \tag{18}$$

wherein $\varepsilon_{1,2}(\boldsymbol{\kappa})$ are two branches of the energy spectrum for a two-dimensional electron gas with SOI.[1]

The addition of $\hat{D}(\boldsymbol{\rho}, z)$ to the wave function $\hat{\Psi}^{(-)}_{01}(\boldsymbol{\rho}, z)$ (15), that is proportional to the potential of the interaction with the defect $\hat{\Psi}^{(-)}_{00}(\boldsymbol{\rho}, z)$, can be written as

$$\hat{\Psi}^{(-)}_{01}(\boldsymbol{\rho}, z) = \frac{2m^*}{\hbar^2}\hat{G}^R_0(\mathbf{r}, \mathbf{r}_0; \varepsilon)(g\hat{\sigma}_0 + \mathbf{J}\hat{\boldsymbol{\sigma}})\hat{\Psi}^{(-)}_{00}(\boldsymbol{\rho}_0, z_0), \tag{19}$$

wherein $\hat{G}^R_0(\mathbf{r}, \mathbf{r}'; \varepsilon)$ is the half-retarded Green's function $z \leq 0$

$$\hat{G}^R_0(\mathbf{r}, \mathbf{r}'; \varepsilon) = \chi_0(z)\chi_0(z')\hat{G}^R_0(\boldsymbol{\rho}, \boldsymbol{\rho}'; \varepsilon), \tag{20}$$

and $\hat{G}^R_0(\boldsymbol{\rho}, \rho'; \varepsilon)$ is the Green's function of a two-dimensional electron gas with SOI.

After the obvious transformations, the wave function $\hat{\Psi}_0^{(-)}(\boldsymbol{\rho}, z)$ (14) can be written in a form that is similar to Equation (15)

$$\hat{\Psi}_0^{(-)}(\boldsymbol{\rho}, z) = \hat{\psi}_s(\boldsymbol{\rho})\chi_0(z), \tag{21}$$

where

$$\hat{\psi}_s(\boldsymbol{\rho}, \boldsymbol{\kappa}; \boldsymbol{\rho}_0) = \hat{\psi}_s^{(00)}(\boldsymbol{\rho}, \boldsymbol{\kappa}) + \frac{2m^*}{\hbar^2}[\chi_0(z_0)]^2(g + \mathbf{J}\hat{\boldsymbol{\sigma}}) \times \hat{G}_0^R(\boldsymbol{\rho}, \boldsymbol{\rho}_0; \varepsilon)\hat{\psi}_s^{(00)}(\rho_o, \boldsymbol{\kappa}) \quad s = 1, 2, \tag{22}$$

and $\boldsymbol{\rho} \neq \boldsymbol{\rho}_0$.

Knowing the wave function of the electrons that passed through the barrier $\hat{\Psi}_{\text{tr}}^{(+)}(\boldsymbol{\rho}, z)$ (13), we can calculate the current through the barrier. At zero temperature and $|eV| \ll \varepsilon_F$, the expression for the tunneling current looks like

$$I = \frac{e^2 V\hbar}{(2\pi)^2 m^*} \times \text{Im} \sum_{s=1,2} \int_{-\infty}^{\infty} d\boldsymbol{\rho} \int_{-\infty}^{\infty} d\boldsymbol{\kappa} \left(\left[\Psi_{s,\text{tr}}^{(+)}(\boldsymbol{\rho}, 0) \right]^* \frac{\partial}{\partial z} \left[\Psi_{s,\text{tr}}^{(+)}(\boldsymbol{\rho}, z) \right]_{z=+0} \right) \times \delta(\varepsilon_F - E_s), \tag{23}$$

in which $\boldsymbol{\kappa}$ is the tangential component of the wave vector, and $E_{1,2}$ is the energy of the two branches of the energy spectrum (18).

Substituting the expression for the wave function $\hat{\Psi}_{\text{tr}}^{(+)}(\boldsymbol{\rho}, z)$ (13) and its derivative into the formula for the tunneling current (23), taking into account the form of the wave function of the "surface" states (21), after integrating with respect to $\boldsymbol{\kappa}'$ we get

$$I = -\frac{e^2 V\hbar k_F^2}{(2\pi)^3 m^*} \left(\frac{\hbar^2 \chi'(0)}{2m^* U_0} \right) \times \sum_{s=1,2} \int_{-\infty}^{\infty} \frac{d\boldsymbol{\rho}}{f(\boldsymbol{\rho})} \int_{-\infty}^{\infty} \frac{d\boldsymbol{\rho}'}{f(\boldsymbol{\rho}')} \frac{j_1 k_F |\boldsymbol{\rho} - \boldsymbol{\rho}'|}{|\boldsymbol{\rho} - \boldsymbol{\rho}'|} \times \int_{-\infty}^{\infty} d\boldsymbol{\kappa} \delta(\varepsilon_F - \varepsilon_0 - \varepsilon_s) \left[\hat{\psi}_s(\boldsymbol{\rho}, \boldsymbol{\kappa}) \right]^* (\hat{\sigma}_0 + \mathbf{M}_0 \hat{\boldsymbol{\sigma}}) \hat{\psi}_s(\rho', \boldsymbol{\kappa}), \tag{24}$$

where $j_1(x)$ is the spherical Bessel function. Accordingly, the tunneling conductance in the linear voltage approximation is equal to $G = I/V$.

For small contacts, $k_F a \ll 1$, Equation (24) is simplified significantly

$$G = \frac{\pi e^2}{\hbar} T_{\text{eff}}(\varepsilon_F) \rho_{3D}(\varepsilon_F) \left[\rho_{2D}(\boldsymbol{\rho}_0) + \left(\mathbf{M}_0 \mathbf{M}_s(\boldsymbol{\rho}_0) \right) \right], \tag{25}$$

wherein $T_{\text{eff}}(\varepsilon_F) \ll 1$ is the effective coefficient of electron tunneling through the barrier

$$T_{\text{eff}}(\varepsilon_F) = \frac{\pi \varepsilon_F \hbar^6 (\pi a^2)^2}{24 m^{*3} U_0^2} \left(\chi_0'(0) \right)^2, \tag{26}$$

$\rho_{3D}^{(0)}$ is the bulk density of states in the halfspace $z > 0$

$$\rho_{3D}^{(0)} = \frac{m^* k_F}{\pi^3 \hbar^2}, \tag{27}$$

$\rho_{2D}(\boldsymbol{\rho}_0)$ and $\mathbf{M}(\boldsymbol{\rho}_0)$ is the local density of states and the local density of magnetization at $\boldsymbol{\rho}_0$

$$\rho_{2D}(\boldsymbol{\rho}_0) = \frac{1}{(2\pi)^2} \sum_{s=1,2} \int_{-\infty}^{\infty} d\boldsymbol{\kappa} \delta(\varepsilon_F - \varepsilon_0 - \varepsilon_s) |\hat{\psi}_s(0, \boldsymbol{\kappa}; \boldsymbol{\rho}_0)|^2,$$

$$\mathbf{M}(\boldsymbol{\rho}_0) = \frac{1}{2(\pi)^2} \sum_{s=1,2} \int_{-\infty}^{\infty} d\boldsymbol{\kappa} \delta(\varepsilon_F - \varepsilon_0 - \varepsilon_s) \tag{28}$$

$$\times \hat{\psi}_s^*(0, \boldsymbol{\kappa}; \boldsymbol{\rho}_0) \hat{\boldsymbol{\sigma}} \hat{\psi}_s(0, \boldsymbol{\kappa}; \boldsymbol{\rho}_0). \tag{29}$$

A similar result was earlier obtained in the Tersoff[13] and Hamann[9] model for a contact between magnetic conductors. For contacts with a diameter $\kappa_F a \geq 1$, where $\kappa_F = \frac{1}{\hbar}\sqrt{2m^*(\varepsilon_F - \varepsilon_0)}$, a more general expression (24) should be used, that accounts for blurred STM images due to the quantum interference of electron waves in the spatially inhomogeneous barrier in the contact region.[40]

Thus, if the area through which the tunneling occurs is small, $\kappa_F a \ll 1$, then the analysis of spatial oscillations of STM conductance is reduced to analyzing the local density of states and local magnetization as a function of the distance from the defect $\boldsymbol{\rho}_0$. In the following sections we will limit ourselves to discussing only LDS and LMD.

3. Wave function and Green's function of surface states with SOI

The Bychkov-Rashba SOI Hamiltonian $\hat{H}_{SO}$ in Equation (5) looks like

$$\hat{H}_{SO} = \frac{\alpha}{\hbar}(\hat{\sigma}_x \hat{p}_y - \hat{\sigma}_y \hat{p}_x), \tag{30}$$

in which α is the SOI constant.

The wave functions of the ideal two-dimensional electron gas with Rashba SOI $\hat{\psi}_s^{(00)}(\boldsymbol{\rho})$ can be written as[1]

$$\hat{\psi}_{1,2}^{(00)}(\boldsymbol{\rho}) = \frac{1}{2\pi\sqrt{2}} e^{i\boldsymbol{\kappa}\boldsymbol{\rho}} \hat{\varphi}_{1,2}(\theta); \quad \hat{\varphi}_{1,2}(\theta) = \begin{pmatrix} 1 \\ \pm i e^{i\theta} \end{pmatrix}, \tag{31}$$

wherein θ is the angle between the direction of the $\boldsymbol{\kappa}$ vector and the x axis, i.e., the phase of the spin part of the wave function $\hat{\varphi}_{1,2}(\theta)$ depends on the direction of the electron wave vector in the xy plane. The eigenvalues of the energy $\varepsilon_{1,2}(\boldsymbol{\kappa})$, corresponding to the wave functions (31), are equal to

$$\varepsilon_{1,2} = \frac{\hbar^2 \kappa^2}{2m^*} \pm \alpha\hbar\kappa > 0. \tag{32}$$

In the following calculations we will assume that the SOI constant is limited by the condition $\alpha < \hbar\kappa_F(2m^*)$.

The Fermi "surface" due to SOI is split into two contours (Fig. 2)

$$\varepsilon_{1,2}(\kappa) = \varepsilon_F - \varepsilon_0 > 0. \tag{33}$$

This results in the removal of spin degeneracy without the occurrence of a gap in the spectrum. The orientation of the

spin in each contour of the Fermi surface (33) is determined by the average

$$\mathbf{s}_{1,2} = \hat{\varphi}^{\dagger}_{1,2}(\theta)\boldsymbol{\sigma}\hat{\varphi}_{1,2}(\theta) = \mp(\sin\theta, -\cos\theta, 0). \tag{34}$$

The vectors $\mathbf{s}_{1,2}$ (34) are perpendicular to the wave vector: $\mathbf{s}_{1,2} \perp \boldsymbol{\kappa} = \kappa(\cos\theta, \sin\theta, 0)$.

We will note a particularity of the energy spectrum (33) that will be useful in discussing the process of scattering by a defect. When the direction of the wave vector reverses, there are two possible states with the same energy. One of them belongs to the same Fermi contour and has a spin that is opposite to the spin of the initial state (for example, states $a \leftrightarrow d$ and $b \leftrightarrow c$ in Fig. 2). The second belongs to another Fermi contour (i.e., it corresponds to another absolute value of the wave vector) and has a spin that is parallel to the spin of the initial state (for example, states $a \leftrightarrow c$ and $b \leftrightarrow d$ on Fig. 2).

We will now write the retarded Green's function for a two-dimensional electron gas with SOI $\hat{G}_0^R(\boldsymbol{\rho}, \boldsymbol{\rho}'; \varepsilon)$,[41] which will be necessary in order to account for the scattering by a defect in the wave function (22)

$$\hat{G}_0^R(\boldsymbol{\rho}, \boldsymbol{\rho}'; \varepsilon) = \frac{im^*}{4\tilde{\kappa}\hbar^2} \times \left\{ \left(\kappa_1 H_0^{(1)}(\kappa_1|\boldsymbol{\rho} - \boldsymbol{\rho}'|) + \kappa_2 H_0^{(1)}(\kappa_2|\boldsymbol{\rho} - \boldsymbol{\rho}'|) \right) \hat{\sigma}_0 - i\hbar \frac{\hat{\sigma}_y(x - x') - \hat{\sigma}_x(y - y')}{|\boldsymbol{\rho} - \boldsymbol{\rho}'|} \right.$$
$$\left. \times \left(\kappa_1 H_1^{(1)}(\kappa_1|\boldsymbol{\rho} - \boldsymbol{\rho}'|) - \kappa_2 H_1^{(1)}(\kappa_2|\boldsymbol{\rho} - \boldsymbol{\rho}'|) \right) \right\}, \tag{35}$$

where

$$\tilde{\kappa} = \sqrt{\frac{2m^*\varepsilon}{\hbar^2} + \left(\frac{m^*\alpha}{\hbar^2}\right)^2}, \tag{36}$$

$$\kappa_{1,2} = \tilde{\kappa} \mp \frac{m^*\alpha}{\hbar^2}. \tag{37}$$

The Green's function (35) contains a divergence at $\boldsymbol{\rho} \to \boldsymbol{\rho}_0$,

$$\hat{G}_0^R(\boldsymbol{\rho}, \boldsymbol{\rho}_0; \varepsilon) \sim \left\{ \frac{\kappa_1}{\kappa_2} \left[1 + \frac{2i}{\pi} \left(\gamma + \ln \frac{\kappa_1|\boldsymbol{\rho} - \boldsymbol{\rho}_0|}{2} \right) \right] \right.$$
$$\left. + \frac{\kappa_2}{\tilde{\kappa}} \left[1 + \frac{2i}{\pi} \left(\gamma + \ln \frac{\kappa_2|\boldsymbol{\rho} - \boldsymbol{\rho}_0|}{2} \right) \right] \right\}. \tag{38}$$

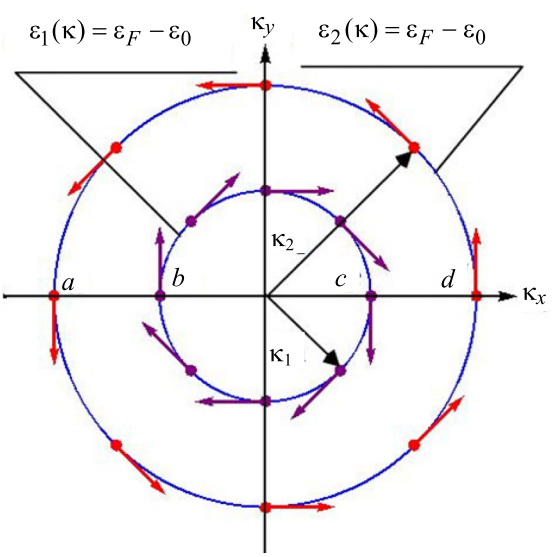

FIG. 2. Two Fermi contours of 2DEG with Rashba SOI. The arrows indicate the direction of the spin.

This divergence leads to a divergence of the wave function (22), which is the result of a "non-physical" selection of the coordinate dependence of the scattering potential (6) in the form of the δ-function. γ is the Euler constant. The asymptotic behavior in (38) allows us to assess the range of applicability of Equation (22), which according to the order of magnitude is determined by the inequality $\kappa_F|\boldsymbol{\rho} - \boldsymbol{\rho}_0| \geq 1$.

By knowing the wave function (31) and the Green's function (35) of an ideal 2DEG with SOI, we can find the wave function (22) in a linear approximation of the scattering potential at the defect (6), which we can use to calculate the LDS (28) and LMD (29).

4. Local density of states

Substituting the wave functions (22) into Equation (28), we find the local density of states. As a result of relatively simple, however rather cumbersome calculations, we get

$$\rho_{2D}(\boldsymbol{\rho}_0) = \frac{m^*}{\pi\hbar^2} \left\{ 1 + \frac{m^{*g}}{4\hbar^2\tilde{\kappa}^2} \left[\left(\kappa_1 J_0(\kappa_1\rho_0) + \kappa_2 J_0(\kappa_2\rho_0) \right) \right.\right.$$
$$\times \left(\kappa_1 Y_0(\kappa_1\rho_0) + \kappa_2 Y_0(\kappa_2\rho_0) \right)$$
$$+ \left(\kappa_1 J_1(\kappa_1\rho_0) + \kappa_2 J_1(\kappa_2\rho_0) \right)$$
$$\left.\left. \times \left(\kappa_1 Y_1(\kappa_1\rho_0) + \kappa_2 Y_1(\kappa_2\rho_0) \right) \right] \right\}, \kappa_{1,2}\rho_0 \geq 1. \tag{39}$$

In Expression (39) and below, the values of $\kappa_{1,2}(\varepsilon)$ and $\tilde{\kappa}(\varepsilon)$ are taken at an energy of $\varepsilon = \varepsilon_F - \varepsilon_0$. Note that Expression (39) does not contain a magnetic input into the LDS, as is the case with the absence of SOI.[19] The result we obtained is in agreement with the conclusions in Ref. 22, and does not confirm the result of Ref. 26, in which the approximation that is linear with respect to SOI constants and exchange interaction of the electrons and the magnetic defect is given a nonzero correction with respect to LDS, proportional to J.

Formula (39) is reduced to the following at large distances from the defect

$$\rho_{2D}(\boldsymbol{\rho}_0) = \frac{m^*}{\pi\hbar^2}\left[1 - \frac{m^* g}{\pi\hbar^2\tilde{\kappa}^2\rho_0}\sqrt{\kappa_1\kappa_2}\cos((\kappa_1+\kappa_2)\rho_0)\right], \quad \kappa_{1,2}\rho_0 \gg 1, \tag{40}$$

where

$$\kappa_1(\varepsilon_F-\varepsilon_0)\kappa_2(\varepsilon_F-\varepsilon_0) = \frac{2m^*(\varepsilon_F-\varepsilon_0)}{\hbar^2},$$
$$\kappa_1(\varepsilon_F-\varepsilon_0)\kappa_2(\varepsilon_F-\varepsilon_0) = 2\tilde{\kappa}(\varepsilon_F-\varepsilon_0) = \sqrt[2]{\frac{2m^*(\varepsilon_F-\varepsilon_0)}{\hbar^2} + \left(\frac{m^*\alpha}{\hbar^2}\right)^2}. \tag{41}$$

Thus, the period of LDS oscillations depends on the sum of the wave vectors $\kappa_{1,2}$ $(\varepsilon_F - \varepsilon_0)$ of two Fermi contours (33)

$$\Delta\rho_0 = \pi/\tilde{\kappa}(\varepsilon_F - \varepsilon_0). \tag{42}$$

Such a conclusion, however, can be made even from the consideration that during the potential scattering in the opposite direction, the electron spin conservation requirement is allowed only by the state belonging to another Fermi contour.[24]

5. Local magnetization density

In cases when the magnetic moment of the defect lies in the plane of the 2DEG with Rashba SOI, the expression for LMD near a magnetic point defect was obtained and analyzed in Ref. 29. Below we examine a more general case, when the magnetic moment of the defect is directed under an arbitrary angle toward the surface plane. The components of the LMD vector, obtained by calculating Formula (29), look like

$$M_x(\boldsymbol{\rho}_0) = -\frac{m^2}{4\pi\hbar^2\tilde{\kappa}^2\rho_0^2}\Big\{\rho_0\big(\kappa_1 J_0(\kappa_1\rho_0) + \kappa_2 J_0(\kappa_2\rho_0)\big) \times \big(J_x\rho_0\big(\kappa_1 Y_0(\kappa_1\rho_0) + \kappa_2 Y_0(\kappa_2\rho_0)\big)$$
$$\times \big(J_z x_0\big(\kappa_1 Y_1(\kappa_1\rho_0) - \kappa_2 Y_1(\kappa_2\rho_0)\big)\big) + \big(\kappa_1 J_1(\kappa_1\rho_0) - \kappa_2 J_1(\kappa_2\rho_0)\big)$$
$$\times \Big[J_z\rho_0 x_0\big(\kappa_1 Y_0(\kappa_1\rho_0) - \kappa_2 Y_0(\kappa_2\rho_0)\big) - \big(J_x\big(x_0^2 - y_0^2\big) + 2J_y x_0 y_0\big)\big(\kappa_1 Y_1(\kappa_1\rho_0) - \kappa_2 Y_1(\kappa_2\rho_0)\big)\Big]\Big\}, \tag{43}$$

$$M_y(\boldsymbol{\rho}_0) = -\frac{m^2}{4\pi\hbar^4\tilde{\kappa}^2\rho_0^2}\Big\{\rho_0\big(\kappa_1 J_0(\kappa_1\rho_0) + \kappa_2 J_0(\kappa_2\rho_0)\big) \times \big(J_y\rho_0\big(\kappa_1 Y_0(\kappa_1\rho_0) + \kappa_2 Y_0(\kappa_2\rho_0)\big) + J_z y_0(\kappa_1 Y_1(\kappa_1\rho_0) - \kappa_2 Y_1(\kappa_2\rho_0))\big)$$
$$+ \big(\kappa_1 J_1(\kappa_1\rho_0) - \kappa_2 J_1(\kappa_2\rho_0)\big) \times [J_z\rho_0 y_0\big(\kappa_1 Y_0(\kappa_1\rho_0) + \kappa_2 Y_0(\kappa_2\rho_0)\big)$$
$$+ \big(J_y\big(x_0^2 - y_0^2\big) + 2J_x x_0 y_0\big)\big(\kappa_1 Y_1(\kappa_1\rho_0) - \kappa_2 Y_1(\kappa_2\rho_0)\big)]\Big\}, \tag{44}$$

$$M_y(\boldsymbol{\rho}_0) = -\frac{m^2}{4\pi\hbar^4\tilde{\kappa}^2\rho_0^2}\Big\{(J_x x_0 + J_y y_0) \times [(\kappa_1 J_1(\kappa_1\rho_0) - \kappa_2 J_1(\kappa_2\rho_0))(\kappa_1 Y_0(\kappa_1\rho_0) + \kappa_2 Y_0(\kappa_2\rho_0))$$
$$+ (\kappa_1 J_0(\kappa_1\rho_0) + \kappa_2 J_0(\kappa_2\rho_0))(\kappa_1 Y_1(\kappa_1\rho_0) - \kappa_2 Y_1(\kappa_2\rho_0))]$$
$$+ J_z\rho_0[(\kappa_1 J_1(\kappa_1\rho_0) - (\kappa_2 J_1(\kappa_2\rho_0))(\kappa_1 Y_1(\kappa_1\rho_0) - \kappa_1 Y_1(\kappa_1\rho_0))$$
$$- (\kappa_1 J_0(\kappa_1\rho_0) + \kappa_2 J_0(\kappa_2\rho_0))(\kappa_1 Y_0(\kappa_1\rho_0) + \kappa_2 Y_0(\kappa_2\rho_0))]\Big\}. \tag{45}$$

As follows from Formulas (43)–(45), in the absence of SOI $M_i(\boldsymbol{\rho}_0)\sim J_i$, which corresponds to a well-known result.[19] We can confirm that

$$M_z(\boldsymbol{\rho}_0, \varepsilon_F) = \rho_\uparrow(\boldsymbol{\rho}_0, \varepsilon_F) - \rho_\downarrow(\boldsymbol{\rho}_0, \varepsilon_F), \tag{46}$$

where $\rho_{\uparrow(\downarrow)}$ $(\boldsymbol{\rho}_0, \varepsilon_F)$ is the LDS for electrons with a spin "up" ("down").

Figures 3 and 4 are composed using Formulas (43)–(45), and illustrate the distribution of local magnetization in the defect region. The charts exclude the region $\kappa_F\rho_0 < 1$ near the point $\rho_0 = 0$, at which our theory is applicable. For comparison, on Fig. 5 we see the LMD in the absence of SOI. Based on Figs. 2–5 we can make the following conclusions: 1. A strong SOI interaction has a significant influence on the LMD distribution $\mathbf{M}(\boldsymbol{\rho}_0)$ near the magnetic defect. 2. The presence of a plane perpendicular to the interface (close to which the surface states are localized), a J_z component of the defect magnetic moment vector $\mathbf{J}$, affects the distribution of the LMD component $\mathbf{M}_{||}(\boldsymbol{\rho}_0)$, which is parallel to the interface, in the presence of SOI (see Figs. 3(a) and 3(b)). In turn, the momentum component $\mathbf{J}_{||}$ that is parallel to the interface, influences the distribution of M_z $(\boldsymbol{\rho}_0)$ (see Figs. 4(b) and 5(b)). In the absence SOI, there is no influence of the $\mathbf{J}$ vector components on the perpendicular components of the LMD vector (see Fig. 5). 3. Even in the case when the $\mathbf{J}$ vector is in the xy plane, the LMD component perpendicular to this plane $M_z(\boldsymbol{\rho}_0)$ is nonzero (see Fig. 4(a)).

Using well-known asymptotes for the Bessel function[42] at $\kappa_{1,2}\rho_0 \gg 1$, we will find the asymptotic expressions for the components of the local density of magnetization vector

$$M_x(\boldsymbol{\rho}_0) = \frac{m^2}{2\pi^2\hbar^4\tilde{\kappa}^2\rho_0^2} \times [x_0 \mathbf{Jn}_{||}^{(0)}(\kappa_1 \cos(2\kappa_1\rho_0) + \kappa_2 \cos(2\kappa_2\rho_0)) + 2y_0\sqrt{\kappa_1\kappa_2}\,\mathbf{Jn}_{\perp}^{(0)} \cos((\kappa_1+\kappa_2)\rho_0) + J_z x_0(\kappa_1 \sin(2\kappa_1\rho_0) - \kappa_2 \sin(2\kappa_2\rho_0))], \quad (47)$$

$$M_y(\boldsymbol{\rho}_0) = \frac{m^2}{2\pi^2\hbar^4\tilde{\kappa}^2\rho_0^2} \times [y_0 \mathbf{Jn}_{||}^{(0)}(\kappa_1 \cos(2\kappa_1\rho_0) + \kappa_2 \cos(2\kappa_2\rho_0)) + 2x_0\sqrt{\kappa_1\kappa_2}\mathbf{Jn}_{\perp}^{(0)} \cos((\kappa_1+\kappa_2)\rho_0) + J_z y_0(\kappa_1 \sin(2\kappa_1\rho_0) - \kappa_2 \sin(2\kappa_2\rho_0))], \quad (48)$$

$$M_z(\boldsymbol{\rho}_0) = \frac{m^2}{2\pi^2\hbar^4\tilde{\kappa}^2\rho_0^2} \times \left[\mathbf{Jn}_{||}^{(0)}(\kappa_1 \sin(2\kappa_1\rho_0) + \kappa_2 \cos(2\kappa_2\rho_0)) + J_z(\kappa_1 \cos(2\kappa_1\rho_0) - \kappa_2 \cos(2\kappa_2\rho_0))\right]. \quad (49)$$

We introduce the following notations for two mutually perpendicular vectors, one of which is directed along the direction of the $\boldsymbol{\rho}_0$, $\mathbf{n}_{||}^{(0)} = \boldsymbol{\rho}_0/\rho_0$ vector, and the second $\mathbf{n}_{\perp}^{(0)}$ perpendicular to it

$$\mathbf{n}_{||}^{(0)} = \mathbf{n}_{||}(\theta_0) = (\cos\theta_0,\ \sin\theta_0, 0),$$
$$\mathbf{n}_{\perp}^{(0)} = \mathbf{n}_{\perp}(\theta_0) = (\sin\theta_0, -\cos\theta_0, 0), \quad \mathbf{n}_{||}\mathbf{n}_{\perp} = 0. \quad (50)$$

In the case when the magnetic moment of the defect is perpendicular to the plane of the interface, $J = J_z$, Formulas (47)–(49) describe the skyrmionic-like spin texture of the electron magnetization around the defect, first investigated theoretically in Ref. 29.

6. Discussion of results

As shown in Ref. 35, the amplitude and period of the oscillations of the density of states and the STM of the conductance at a distance of $\boldsymbol{\rho}_0$ from the defect, are determined by electron interference, the wave vectors of which before and after defect scattering are collinear to the $\boldsymbol{\rho}_0$ vector. In order to explain the obtained results (47)–(49), we will examine the matrix elements of the magnetic interaction of the electron with the defect, which determine the probability of backscattering. An electron, approaching a defect at an angle θ with respect to the x axis, with the wave vector $\boldsymbol{\kappa}$, corresponds to an electron moving in the opposite direction with the wave vector $-\boldsymbol{\kappa}$, with an angle $\theta + \pi$ with respect to the x axis. The matrix elements $\hat{\varphi}_{1,2}^{\dagger}(\theta)\mathbf{J}\boldsymbol{\sigma}\hat{\varphi}_{1,2}(\theta+\pi)$ of the transition between states belonging to the same Fermi surface contour, are equal to[43]

$$\hat{\varphi}_{1,2}^{\dagger}(\theta)\mathbf{J}\boldsymbol{\sigma}\hat{\varphi}_{1,2}(\theta+\pi) = J_z \mp i(J_x\cos\theta + J_y\sin\theta) = J_z \mp i\mathbf{Jn}_{||}(\theta), \quad (51)$$

whereas the matrix elements $\hat{\varphi}_{1,2}^{\dagger}(\theta)\mathbf{J}\boldsymbol{\sigma}\hat{\varphi}_{1,2}(\theta+\pi)$ of the transition between states belonging to different Fermi surface contours, look like

$$\hat{\varphi}_{1,2}^{\dagger}(\theta)J\sigma\hat{\varphi}_{2,1}(\theta+\pi) = \pm(J_y\cos\theta - J_x\sin\theta) = \mp\mathbf{Jn}_{\perp}(\theta). \quad (52)$$

Equations (51) and (52) reflect the fact that the probability of backscattering depends on the projection of the electron spin direction $\mathbf{s}_{1,2}(\boldsymbol{\kappa})||\ \mathbf{n}_{\perp}(\theta)$ (34) in the direction of the magnetic moment of the defect $\mathbf{J}$.

Expressions (51) and (52) explain the dependence of the vector components $\mathbf{M}(\boldsymbol{\rho}_0)$ on the direction of the magnetic moment of the defect $\mathbf{J}$.

The terms proportional to the projection of the magnetic moment of the impurity on the direction of the spin $\mathbf{Jn}_{\perp}$, describe the input of the no spin-flip scattering process into

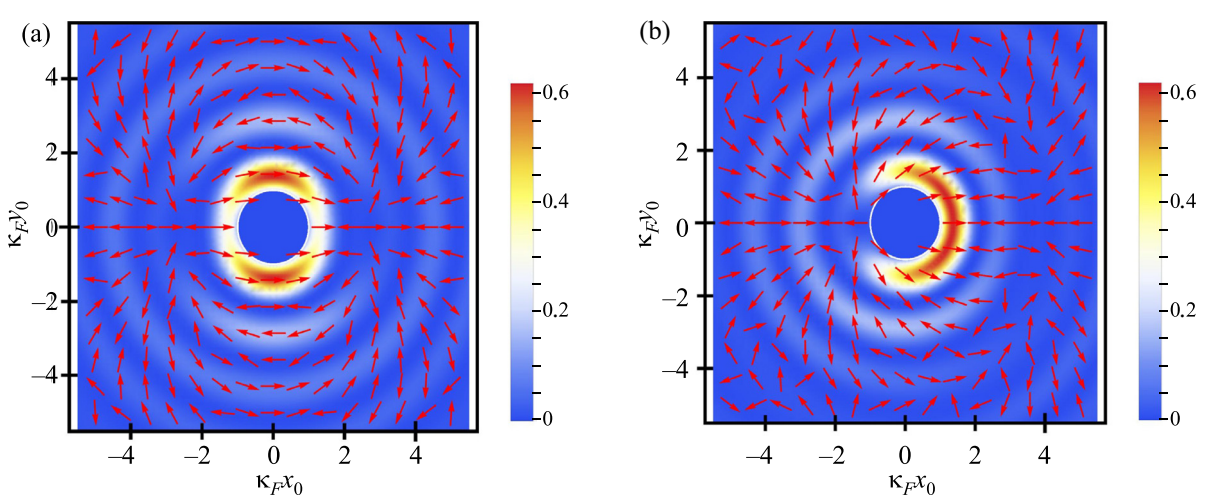

FIG. 3. The distribution of the magnetization density $M_x^2 + M_y^2$ in the xy plane. $\mathbf{J} = J(1,0,0)$ (a); $\mathbf{J} = J(1/\sqrt{2}, 0, 1/\sqrt{2})$ (b), arrows show the directions of the vector $\mathbf{M}_{||}(M_x, M_y)$; $m^*\alpha/\kappa_F\hbar^2 = 0.3$.

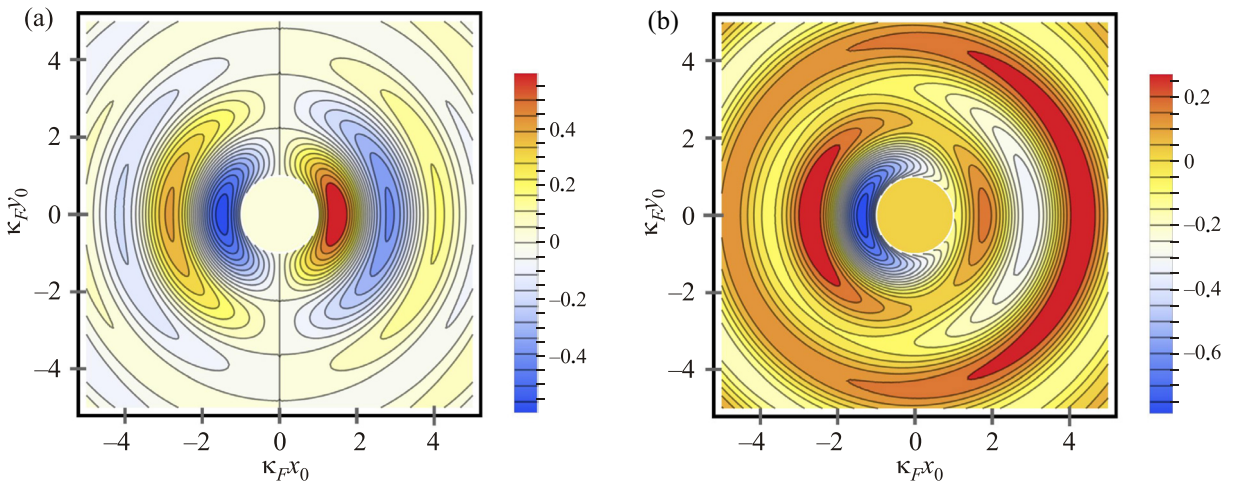

FIG. 4. Spatial distribution of the M_z component in units $m^{*2}J/4\pi\hbar^4$; $m^*\alpha/\kappa_F\hbar^4 = 0.3$: $\mathbf{J} = J(1,0,0)$ (a); $\mathbf{J} = J(1/\sqrt{2}, 0, 1/\sqrt{2})$ (b).

the $\mathbf{M}(\boldsymbol{\rho}_0)$ vector, which is accompanied by transitions between energy spectrum branches. The corresponding term in LMD oscillations as a function of the distance $\boldsymbol{\rho}_0$, depends on the sum of Fermi wave vectors for two energy bands (42), as is the case for LDS oscillations (40).

The terms proportional to vector components $\mathbf{J}\mathbf{n}_{||}$ and J_z of the defect magnetic moment $\mathbf{J}$, which are perpendicular to $\mathbf{s}_{1,2}$, take into account the spin-flip scattering. The periods of these harmonics in the LDS depend on the radii of each of the Fermi surface contours, separately

$$\Delta\rho_0^{(1,2)} = \pi/\kappa_{1,2}(\varepsilon_F). \tag{53}$$

In accordance with this substantially isotropic distribution of local magnetization $\mathbf{M}(\boldsymbol{\rho}_0)$, the most convenient oscillation analysis is in the $\boldsymbol{\rho}_0$ direction, which is parallel to the projection $\mathbf{J}_{||}$ of the $\mathbf{J}$ vector on the xy plane. With this type of geometry, $\mathbf{J}\mathbf{n}_\perp = 0$ and $\mathbf{J}\mathbf{n}_{||} = J_{||} = (J^2{}_x + J^2{}_y)^{1/2}$, and the amplitude of the oscillations with periods (53) is maximized. Knowing the periods $\Delta\rho_0^{(1,2)}$ of the spatial oscillations of the $\mathbf{M}(\boldsymbol{\rho}_0)$ vector components, caused by spin-flip scattering, we can define the SOI constant

$$\frac{1}{\Delta\rho_0^{(2)}} - \frac{1}{\Delta\rho_0^{(1)}} = \frac{2m^*\alpha}{\pi\hbar^2}. \tag{54}$$

Note that the eigenstates and the wave functions are also known for the Dresselhaus Hamiltonian of SOI[44] (see Ref. 1, for example)

$$\hat{H}_{SOD} = \frac{\beta}{\hbar}\left(\hat{\sigma}_x\hat{p}_x - \hat{\sigma}_y\hat{p}_y\right), \tag{55}$$

wherein β is the SOI constant. They allow us to obtain analytic expressions for Green's function for 2DEG on an unbounded plane, similar to Expression (35), and calculate the spatial distribution for LDS and LMD around the magnetic defect. Despite the fact that the Hamiltonian in (55) has a different symmetry in comparison to the Bychkov-Rashba Hamiltonian (30), the final results differ from the ones obtained above in Section 5, due to the substitutions in Formulas (43)–(45) $x_0 \to y_0$, $y_0 \to x_0$, $\alpha \to \beta$, and also due to the substitution

$$\begin{aligned} &\mathbf{n}_{||}^{(0)} \to \mathbf{n}_{||}^{(0)} = (\sin\theta_0, \cos\theta_0, 0), \\ &\mathbf{n}_\perp^{(0)} \to \mathbf{n}_\perp^{(0)} = (\cos\theta_0, -\sin\theta_0, 0), \mathbf{n}_{||}^{(0)}\mathbf{n}_\perp^{(0)} = 0, \end{aligned} \tag{56}$$

in Formulas (47)–(49).

All conclusions presented in this section, relative to the LDS and LMD distributions, remain valid for the Dresselhaus

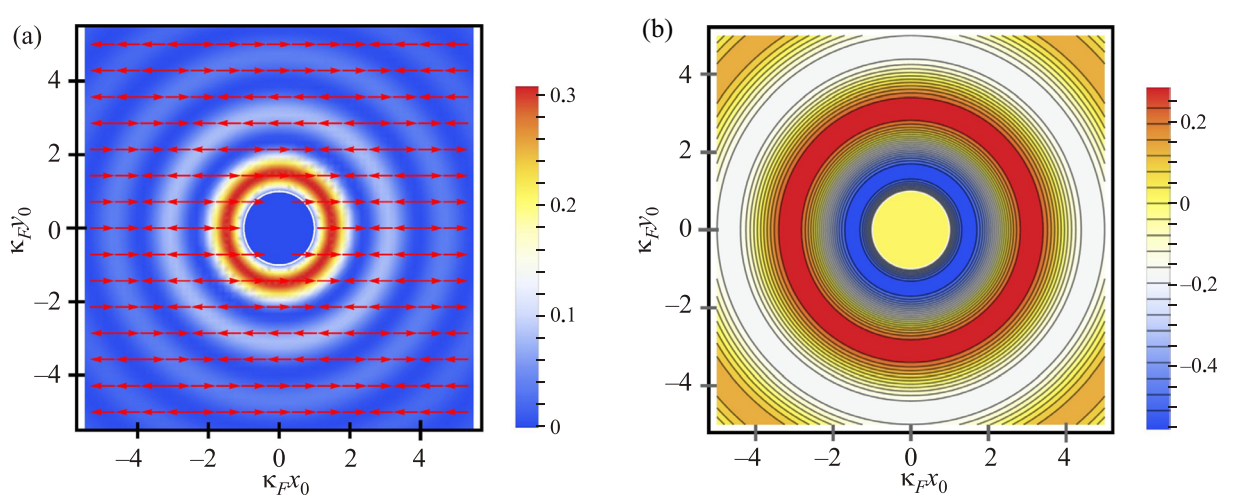

FIG. 5. The distribution of the magnetization density $M_x^2 + M_y^2$ in the xy plane (a) and M_z components perpendicular to the interface (b) in units $m^{*2}J/4\pi\hbar^4$ in the absence of SOI, $\alpha = 0$; $\mathbf{J} = J(1/\sqrt{2}, 0, 1/\sqrt{2})$; arrows show the directions of the $\mathbf{M}_{||} = (M_x, M_y)$ vector.

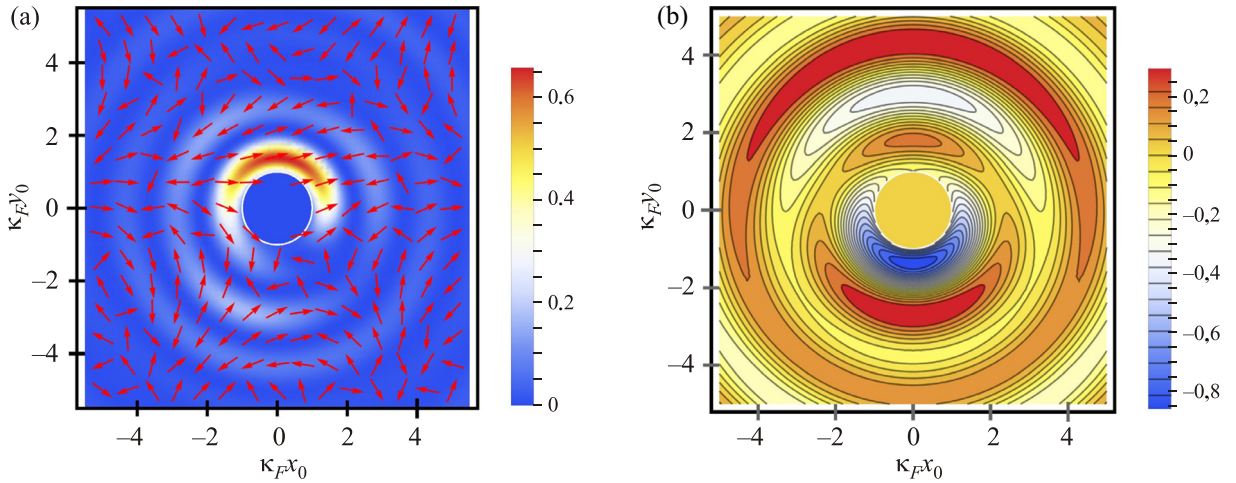

FIG. 6. The distribution of magnetization density $M_x^2 + M_y^2$ in the xy plane (a) and M_z components perpendicular to the interface (b) in units $m^{*2}J/4\pi\hbar^4$ with Dresselhaus SOI (55) $m^*\beta/\kappa_F\hbar^2 = 0.3$; $\mathbf{J} = J(1/\sqrt{2}, 0, 1/\sqrt{2})$; the arrows indicate the direction of the $\mathbf{M}_{||} = (M_x, M_y)$ vector.

SOI, even though the concrete distribution of the absolute value and direction of the LMD vector changes significantly, as illustrated by Fig. 6 (compare Figs. 3(b) and 4(b), and Figs. 6(a) and 6(b)).

Conclusion

In this study we have generalized the model of an inhomogeneous δ-barrier[32] for a case of a potential barrier consisting of magnetic dielectrics (1). We examined tunneling between quasi-two-dimensional (surface) states and bulk states. For a large amplitude of the barrier, an expression for the tunneling current through the contact (24), that can be used to describe SP-STM experiments, is obtained. It is shown that in the case when the typical size of the tunneling field is significantly smaller than the de Broglie electron wavelength $\lambda\!\!\!^{-}_F = 1/\kappa_F$, the conductance of the contact is proportional to the scalar product of a specific magnetization barrier and the local magnetization of 2DEG (25). The result in (25) is similar to the results from Ref. 13, in which the conductance of the SP-STM conductance is calculated when tunneling occurs between two ferromagnetic conductors, within the framework of the Tersoff and Hamann model.[9] We examine a case when the inhomogeneous magnetization in 2DEG with SOI is associated with the presence of a single magnetic defect. Within the framework of the Born approximation, we found the dependence of the local density of states and local magnetization of 2DEG, on the distance between the contact and the defect (39), (43)–(49). At large distances $\kappa_F\rho_0 \gg 1$ we obtained asymptotic expressions for $\rho_{2D}(\boldsymbol{\rho}_0)$ and $\mathbf{M}(\boldsymbol{\rho}_0)$ (40), (47)–(49). It is shown that the study of SP-STM images showing spatial oscillations of the conductance allows us to determine the SOI constant (54).

In conclusion, one of the authors (Yu. K.) wishes to thank A. A. Zvyagin, G. P. Mikitik, and A. N. Omelyanchyk for the useful discussions.

[a)]Email: kolesnichenko@ilt.kharkov.ua

[1]R. Winkler, *Spin–Orbit Coupling Effects in Two-Dimensional Electron and Hole Systems* (Springer-Verlag, Berlin, Heidelberg, 2003).
[2]D. Bercioux and P. Lucignano, Rep. Prog. Phys. **78**, 106001 (2015).
[3]D. Awschalom and N. Samarth, Physics **2**, 50 (2009).
[4]G. Nicolay, F. Reinert, and S. Hufner, Phys. Rev. B **65**, 033407 (2001).
[5]G. Bihlmayer, Yu. M. Koroteev, P. M. Echenique, E. V. Chulkov, and S. Blugel, Surf. Sci. **600**, 3888 (2006).
[6]A. Tamai, W. Meevasana, P. D. C. King, C. W. Nicholson, A. de la Torre, E. Rozbicki, and F. Baumberger, Phys. Rev. B **87**, 075113 (2013).
[7]S. LaShell, B. A. McDougall, and E. Jensen, Phys. Rev. Lett. **77**, 3419 (1996).
[8]C. Bai, *Scanning Tunneling Microscopy and its Applications* (Springer Verlag, New York, 2000).
[9]J. Tersoff and D. R. Hamann, Phys. Rev. Lett. **50**, 1998 (1983).
[10]J. Bardeen, Phys. Rev. Lett. **6**, 57 (1961).
[11]M. Bode, Rep. Prog. Phys. **66**, 523 (2003).
[12]R. Wiesendanger, Rev. Mod. Phys. **81**, 1495 (2009).
[13]D. Wortmann, S. Heinze, Ph. Kurz, G. Bihlmayer, and S. Blügel, Phys. Rev. Lett. **86**, 4132 (2001).
[14]J. Friedel, Nuovo Cimento **7**, 287 (1958).
[15]M. F. Crommie, C. P. Lutz, and D. M. Eigler, Nature **363**, 524 (1993); Science **262**, 218 (1993).
[16]L. Petersen, Ph. Hofmann, E. W. Plummer, and F. Besenbacher, J. Electron Spectrosc. Relat. Phenom. **109**, 97 (2000).
[17]L. Simon, C. Bena, F. Vonau, M. Cranney, and D. Aube, J. Phys. D: Appl. Phys. **44**, 464010 (2011).
[18]N. V. Khotkevych-Sanina, Yu. A. Kolesnichenko, and J. M. van Ruitenbeek, New J. Phys. **15**, 123013 (2013).
[19]C. Kittel, *Quantum Theory of Solids* (John Wiley & Sons, Inc., New York, 1963).
[20]O. Pietzsch, S. Okatov, A. Kubetzka, M. Bode, S. Heinze, A. Lichtenstein, and R. Wiesendanger, Phys. Rev. Lett. **96**, 237203 (2006).
[21]R. Chirla, C. P. Moca, and I. Weymann, Phys. Rev. B **87**, 245133 (2013).
[22]A. Stróżecka, A. Eiguren, and J. I. Pascual, Phys. Rev. Lett. **107**, 186805 (2011).
[23]H.-M. Guo and M. Franz, Phys. Rev. B **81**, 041102R (2010).
[24]L. Petersen and P. Hedegard, Surf. Sci. **459**, 49 (2000).
[25]J. I. Pascual, G. Bihlmayer, Yu. M. Koroteev, H.-P. Rust, G. Ceballos, M. Hansmann, K. Horn, E. V. Chulkov, S. Blügel, P. M. Echenique, and Ph. Hofmann, Phys. Rev. Lett. **93**, 196802 (2004).
[26]A. V. Balatsky and I. Martin, Quantum Inf. Process. **1**, 355 (2002).
[27]S. M. Badalyan, A. Matos-Abiague, G. Vignale, and J. Fabian, Phys. Rev. B **81**, 205314 (2010).
[28]J. Fransson, Phys. Rev. B **92**, 125405 (2015).
[29]S. Lounis, A. Bringer, and S. Blugel, Phys. Rev. Lett. **108**, 207202 (2012).
[30]N. V. Khotkevych, Yu. A. Kolesnichenko, and J. M. van Ruitenbeek, e-print arXiv:1601.03154.
[31]E. I. Rashba, Fiz. Tverd. Tela **2**, 1224 (1960) [Sov. Phys. Solid State **2**, 1109 (1960)], Yu. Bychkov and E. I. Rashba, JETP Lett. **39**, 78 (1984).
[32]I. O. Kulik, Yu. N. Mitsai, and A. N. Omel'yanchuk, Sov. Phys.-JETP **39**, 514 (1974) [Zh. Eksp. Theor. Phys. **66**, 1051 (1974)].
[33]Ye. S. Avotina, Yu. A. Kolesnichenko, and J. M. van Ruitenbeek, Fiz. Nizk. Temp. **36**, 1066 (2010) [Low Temp. Phys. **36**, 849 (2010)].
[34]Ye. S. Avotina, Yu. A. Kolesnichenko, and J. M. van Ruitenbeek, Phys. Rev. B **80**, 115333 (2009).
[35]N. V. Khotkevych-Sanina, Yu. A. Kolesnichenko, and J. M. van Ruitenbeek, New J. Phys. **15**, 123013 (2013).
[36]N. V. Khotkevych and Yu. A. Kolesnichenko, Phys. J. **1**, 35 (2015).
[37]A. A. Zvyagin and H. Johannesson, Phys. Rev. Lett. **81**, 2751 (1998).

[38]N. V. Khotkevych, Yu. A. Kolesnichenko, and J. M. Ruitenbeek, Fiz. Nizk. Temp. **39**, 384 (2013) [Low Temp. Phys. **39**, 299 (2013)].
[39]A. Messia, *Quantum Mechanics* (Nauka, Moscow, 1978), Vol. 1.
[40]N. V. Khotkevych-Sanina and Yu. A. Kolesnichenko, Physica E **59**, 133 (2014).
[41]A. Csordrás, J. Cserti, A. Prályi, and U. Zëulicke, Eur. Phys. J. B **54**, 189 (2006).
[42]G. Korn and T. Korn, *Mathematical Handbook* (McGraw-Hill, New York, 1968).
[43]A. A. Abrikosov, *Fundamentals of the Theory of Metals* (Fizmatlit, Moscow, 2009).
[44]G. Dresselhaus, Phys. Rev. **100**, 580 (1955).

Translated by A. Bronskaya